

DMC GEOMETRIC PERFORMANCE ANALYSIS

R.Alamús^a, W.Kornus^a, I.Riesinger^b

^a Cartographic Institute of Catalonia (ICC), Barcelona, Spain - (ramon.alamus; wolfgang.kornus)[@icc.cat](mailto:icc.cat)

^b Chair for Photogrammetry and Remote Sensing, Technical University Munich, Germany - isabell-riesinger@web.de

KEY WORDS: Geometric calibration, Digital camera, Accuracy

ABSTRACT

Since the apparition of the first large format digital aerial cameras there are great expectations on their performance. The dream to get aerial images virtually free of geometric errors and with a greater radiometric quality is nearly going to be fulfilled. Nevertheless, some reports on systematic image residuals (Honkavaara et al., 2006a and 2006b, Alamús et al., 2005 and 2006, Cramer, 2007), unexpected height errors in aerotriangulation and the need for additional self-calibration parameters (Alamús et al., 2005, Cramer, 2007) have been reported since 2005.

In this paper a preliminary analysis on the theoretical accuracies of the ZEISS/INTERGRAPH (Z/I) Digital Metric Camera (DMC) and analogue camera in aerotriangulation is carried out. This analysis considers a mathematical model where the image has conical geometry and it is free of systematic errors. It is studied the influence of the base-to-height ratio, the image pointing precision (manual and automatic), as well as, tie point density and distribution (classical Von Gruber distribution or high, dense and uniform distribution) and GPS observations for projection centre. The expected accuracy in the case of the aerotriangulation of analogue images using “current” aerotriangulation set up (the a priori accuracy for image pointing, ground control measurement and GPS and tie point distribution) is computed. Then, a minimum aerotriangulation set up for the DMC camera is derived in order to warranty the same, or even better, theoretical accuracy level that is obtained in aerotriangulation with analogue images.

ICC experiences have proven that the expected theoretical accuracy in aerotriangulation is sometimes hard to obtain without considering an appropriate self-calibration parameter set in the bundle block adjustment. As it is well known that additional self-calibration parameters absorb error propagation effects, which can be caused by non modelled systematic error sources. Some authors (Alamús et al., 2006 and E. Honkavaara, et al. 2006b) have detected systematic residuals in the order of one tenth of a pixel rms (root mean squared) in DMC image space. Investigations on the systematic error characterization, distribution in image space and stability over time and flying height are carried out.

Finally conclusions are drawn from the investigations.

1. INTRODUCTION

In 2004 and 2005 the Institut Cartogràfic de Catalunya (ICC) acquired two digital ZEISS/INTERGRAPH (Z/I) Digital Metric Cameras (DMC). Since the beginning height accuracy at check points were not always as good as expected, despite the great radiometric and geometric performance of the cameras. Some authors (Schroth 2007, Alamús et al., 2006) have reported unexpected large errors in height.

The DMC camera simultaneously captures a high resolution panchromatic images of 13 824 x 7 680 pixels (across-track and along-track respectively) and four multi-spectral images (red, green blue and near infrared) of 3 072 x 2 048 pixels. The high resolution image is formed from the four images acquired with four inclined panchromatic high resolution camera heads with a focal length of 120 mm. Each of these camera heads is covering a quarter of the final image, called virtual image. The four low resolution multi-spectral images in the colour bands red, green, blue and near-infrared are acquired by four additional nadir looking camera heads with a focal length of 25 mm. The four images completely cover the virtual high resolution image. (See Hinz, 1999; Zeitler et al., 2002; Dörstel et al., 2003 for details.)

In this paper firstly the theoretical accuracy is assessed, which is expected from photogrammetric point determination with DMC in comparison to analogue cameras. Secondly, it is proved that in reality, at least under some conditions, height accuracy is worse than expected, which, however, can be compensated to a large extent by applying a suitable self-

calibration approach. Finally, remaining systematic errors in the image space are analyzed.

2. ON THE THEORETICAL ACCURACY

In this section the theoretical height accuracy derived from bundle block adjustment with DMC images is analyzed using simulations. Main interest of the authors in this section is error propagation through the block instead an analysis of height accuracy in a single model. The influence of the following four parameters are investigated: 1) base-to-height ratio (b/h), 2) image observation accuracy, 3) GPS observation accuracy and 4) image point distribution (and density). The goal is to assess the conditions in aerotriangulation, which are required to reach the same or even a higher level of precision compared to the results of aerotriangulations with analogue cameras.

In a first step several simulations are performed considering the four different camera characteristics described in table 1: An analogue camera, two cameras with some features of the DMC but with b/h of 0.60 and 0.47 and finally the DMC with a b/h of 0.31. BH_47 represents a fictitious camera with an intermediate b/h value, which shall help to better understand the accuracy degradation from $b/h = 0.60$ (analogue) to $b/h = 0.31$ (DMC).

In order to simplify the analysis on the theoretical accuracy the simulation are based on a single image strip of 5 km length with four ground control points (GCP) at the four corners. A conventional Von Gruber point distribution scheme of three tie points is assumed, resulting in 3 point rows located at the borders and in the centre of the strip. The flying height is

1000 m, the ground sampling distance (GSD) 10 cm and the endlap 60% in all simulations.

Camera	Focal length [mm]	Pixel size [μm]	# pixels columns x rows	B/H
Analogue	150	15	15000x15000	0.60
BH_60	120	12	15000x15000	0.60
BH_47	120	12	11776x13824	0.47
DMC	120	12	7680x13824	0.31

Table 1. Camera features used in simulation (pixel size for the analogue camera represents the scanning size)

2.1 Influence of base-to-height ratio

In general, large format frame-based aerial digital cameras have to reduce their b/h due to design or construction restriction. The standard value of 0.60 that is used to analogue images from aerial metric cameras is reduced to 0.31 in the case of the DMC. In this sub-section the influence of the b/h on the theoretical height accuracy is analyzed. Weighting for image observations is set to 5 μm for the analogue camera, and to 2 μm for the BH_60, BH_47 and DMC cameras. GCP weighting is set to 4 cm in planimetry and to 6 cm in altimetry. No GPS observations are included in the simulations.

In figure 1 the standard deviations in height for the tie points, which are located in the strip centre, are plotted. There are two major effects to be noticed:

- The height accuracy degrades along with the reduction of the b/h and is the worse for the DMC.
- The deterioration of the height accuracy due to the small b/h of the DMC cannot be compensated even by an image observation accuracy, which is twice as high (2 μm corresponds to 1/6th of a pixel) than for the analogue camera (5 μm corresponds to 1/3rd of a pixel; see also the accuracies corresponding to the BH_60, BH_47 and DMC in figure 2).

Despite from equation (1) it is derived that in a model the reduction of b/h by a factor of 2 is compensated by improving the image pointing accuracy by a factor of 2, the assessment b) does not contradict the theory because equation (1) is related to the accuracy in height within a single model, meanwhile analysis carried out in this section is related to the error propagation through the block in aerotriangulation. It must be noticed in fig. 1 that in the neighbourhood of GCP at Km 0 analogue and DMC simulations have height accuracies consistent with eq. (1).

$$\sigma_H = \sqrt{2} \frac{h^2}{bf} \sigma_i \quad (1)$$

where f focal length
 h flying height
 b base
 σ_i accuracy in image space
 σ_H accuracy in height

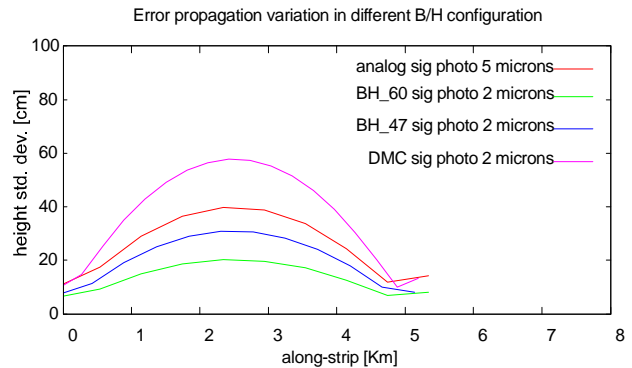


Figure 1. Influence of b/h on the theoretical height accuracies of the tie points located in the strip centre

In other words: The deterioration of the height accuracy due to the half b/h (e.g. DMC compared to an analogue camera) cannot only be compensated by double image pointing accuracy.

2.2 Influence of image observation accuracy

In this sub-section the influence of the image observation accuracy on the theoretical height accuracy is analyzed. Weighting for image observations is set to 5 μm (ground control and tie points) for the analogue camera. In the case of the DMC it is set to 4 μm for GCP observations and, varying from 1.2 to 2.5 μm , for tie point observations. GCP weighting is set to 4 cm in planimetry and to 6 cm in altimetry. No GPS observations are included in the simulations.

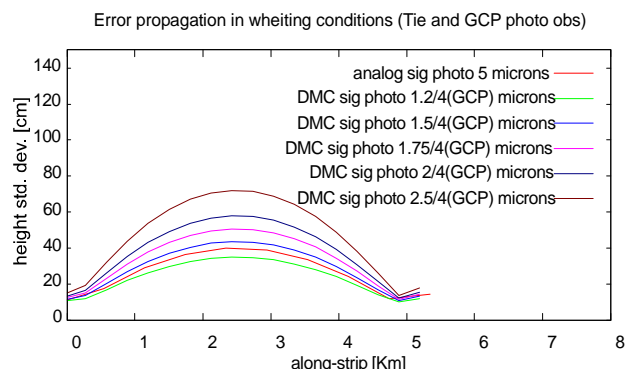


Figure 2. Influence of image observation accuracy on the theoretical height accuracies of the tie points located in the strip centre

The results in figure 2 point out, that an observation accuracy between 1.2 and 1.5 μm in DMC images is required to achieve a comparable height accuracy in simulation set up, which would be obtained with 5 μm observation accuracy in analogue images. According to our experience semi manual tie point measurement can reach an image pointing accuracy in the level of 0.2 pixel (2.4 μm) and automatic tie point matching accuracy a level of 0.1 pixel size (1.2 μm) (Alamús et al., 2005).

In other words: In the simulations set up the lower b/h of the DMC can theoretically be compensated with an image pointing accuracy in the level of 1.2 to 1.5 μm . Such pointing accuracy is only achievable by means of automatic image matching techniques.

It has not to be discarded that error propagation depends on image pointing accuracy and GCP accuracy (as initial

conditions in the adjustment) and distance (i.e. number of images) between GCP. In other words: The larger the distance between GCP is, the higher is the required image pointing accuracy to keep DMC height accuracy (due error propagation) comparable to analogue case.

2.3 Influence of GPS observation accuracy

In this sub-section the influence of the GPS observation accuracy on the theoretical height accuracy is analyzed. Weighting for image observations is set to 5 μm (ground control and tie points) for the analogue camera. In the case of cameras BH_60 and DMC it is set to 4 μm for GCP observations and 1.75 μm for tie point observations. GCP weighting is set to 4 cm in planimetry and to 6 cm in altimetry. Weighting for the GPS observations is set to 10 cm, 5 cm and 2.5 cm in three different simulations including a linear drift parameter set, which is introduced with low weight (50 m).

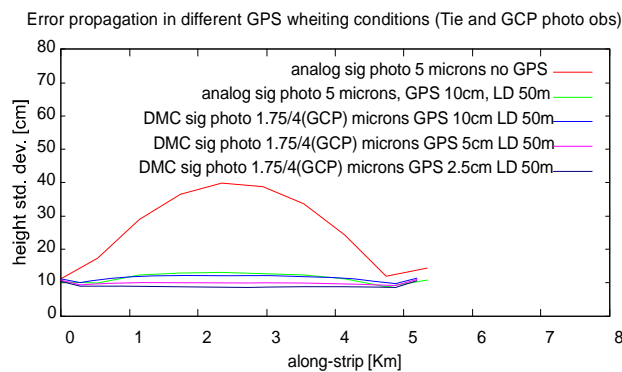


Figure 3. Influence of GPS observation accuracy on theoretical height accuracies of tie points located in the strip centre

Figure 3 shows that the difference in height accuracy obtained for the DMC and the analogue camera in sub-section 2.1 disappears, if GPS observations are available. GPS weight settings of 10 cm lead to the same level of theoretical height accuracy for both the DMC and for the analogue camera.

2.4 Influence of image point distribution

In this sub-section the influence of a high dense photogrammetric network (that, in practice, could be obtained by automatic aerotriangulation procedures) versus the conventional Von Gruber distribution on the theoretical height accuracy is analyzed. In these simulations a dense distribution of 80 tie points per image distributed in the zones of Von Gruber has been considered in addition to the conventional Von Gruber point distribution scheme of three tie points. Weighting for image observations is set to 5 μm (ground control and tie points) for the analogue camera. In the case of the DMC it is set to 4 μm for GCP observations and 1.75 μm for tie point observations. GCP weighting is set to 4 cm in planimetry and 6 cm in altimetry. No GPS observations are included in the simulations.

The results in figure 4 show that a dense photogrammetric network, as it can be obtained by automatic image matching techniques, can also contribute to compensate the lower height accuracy caused by the smaller b/h of the DMC achieving height accuracies comparable to the obtained results using GPS observations shown in figure 3.

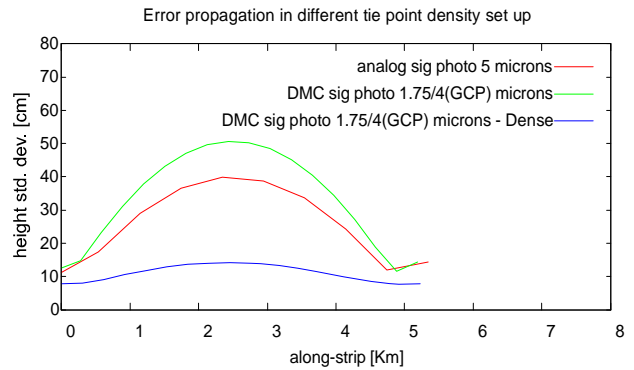


Figure 4. Influence of image point distribution on theoretical height accuracies of tie points located in the strip centre

A comparison to the analogue image case using a dense tie point distribution has not been considered by the time of data compilation. Further work should complete the analysis in this direction.

3. ON DMC PRACTICAL EXPERIENCES

Some authors (Alamús et al, 2005 and 2006 and Schroth, 2007) have already reported that DMC block aerotriangulations generate larger height errors than predicted by (Dörstel, 2003). Recent studies relate these height errors to systematic errors in the DMC image space (Alamús et al., 2006 and E. Honkavaara, et al. 2006b). The need for additional parameters, which compensate these unmodelled systematic errors in image space, is currently discussed in the community (Alamús et al., 2006, Cramer 2007). Preliminary results on the capability of 4 sets of 12 self-calibration parameters to overcome with the unexpected large error in height are discussed. In this section the detected systematic errors in image space are analyzed using real data of the test block Rubí

3.1 DMC accuracy in Rubí block

The Rubí block was acquired 8th of March 2005. It consists of 426 images distributed in 13 parallel and 3 transversal strips, taken at a flight altitude of 1000 m above ground level, which corresponds to a GSD of 10 cm. 19 natural GCP as well as GPS/INS data for all 426 images were used to aerotriangulate the block. Moreover, 20 well distributed check points were measured in the images, which belong to the fourth order Geodetic Network of Rubí and have an accuracy of 2 cm in planimetry and 4 cm in altimetry.

Aerotriangulation.	No. image obs.	No. object points
AT 1	45462	7762
AT 2	25959	4152
AT 3	32858	4683
AT 4	187810	34695

Table 2. Number of image observations and corresponding number of object points for the 4 different aerotriangulation performed in Rubí Block

In four different aerotriangulations (AT1-AT4) the number of object points and image observations were varied (see table 2) using the same ground control and check point observations. Images used in AT 1 were processed with DMC Post-Processing Software (PPS) version 4.4. Images used in AT 2, AT 3 and AT 4 were processed with the PPS version 5.1. Since the upgrade from version 4.4 to 5.1 implies a difference in

geometry, it was not possible to use the same observations of AT 1. The geometry of version 5.0 and older is related to the mid exposure time meanwhile version 5.1 geometry is related to the beginning of the exposure instead. This upgrade improves the GPS time synchronization, but causes a shift in the image (between version 5.1 and the older ones), which corresponds to the half size of the forward motion compensation (Hefele & Dörstel, 2007).

It has to be noticed that AT 1 and AT 2 are comparable in terms of block connection. Despite AT 2 has a smaller number of image observations and corresponding object points than AT 1, they are better distributed and the average of images connected by an object point is larger in AT 2 than in AT 1. Because of that, AT 2 compensates the minor number of points with better connected points leading to comparable block connection to AT 1.

The bundle block adjustments have been computed using 10 cm *a priori* GPS accuracy and 2 μm *a priori* image pointing accuracy. Notice that 10 cm *a priori* accuracy for GPS has been a “standard” at the ICC in analogue data sets, and, according to results of sections 2.2 and 2.3, using this weighting configuration it should be expected comparable results to the analogue data sets up to now. The four aerotriangulations have been calculated twice: without any additional parameter set and with one set of 12 self-calibration parameters per image quarter (4 sets of 12 parameters in total) (see Alamús et al., 2006). Figure 5 summarizes the height accuracies obtained at the 20 check points. Three conclusions can be drawn from the results:

1. The results obtained without additional parameters (in the background) are the worse the better the block connection is established (which is, usually, but not necessarily, related to a larger number of image observations and corresponding object points). Similar effects are also described by (Schroth, 2007), who shows significantly larger height residuals at check points in a block with an 80% sidelap than in the same block with 60% sidelap or less.
2. The results obtained with 4 sets of 12 self-calibration parameters computations keep the same level of height accuracy almost independently of block redundancy.
3. The results obtained for AT1 and AT2 are comparable in both computations (with and without additional parameters), which indicates, that image geometry change due to the version upgrade does not affect significantly the adjustment results.

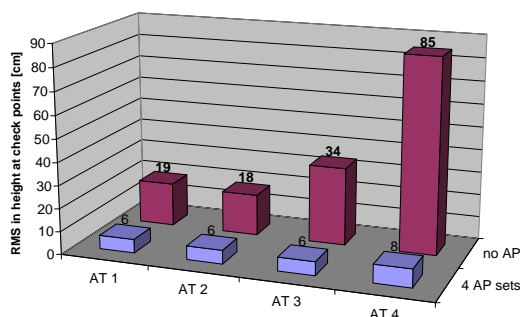


Figure 5. Height accuracy dependency on redundancy and number of observations and redundancy using additional parameters or none

Figure 6 shows the combined effect of varying the weights of GPS and image observations without using self-calibration. The height accuracy at the check points increases along with decreasing weights of image observations. Highly weighted GPS observations (2.5 cm, 1- σ) and lowly weighted image observations (6 μm , 1- σ) lead to similar good results as achieved with lowly weighted GPS observations (10.0 cm, 1- σ), highly weighted image observations (2 μm , 1- σ) and 4 sets of 12 self-calibration additional parameters. In this case the block geometry is fixed by the GPS and the image observations will get higher residuals, which otherwise are absorbed by self-calibration.

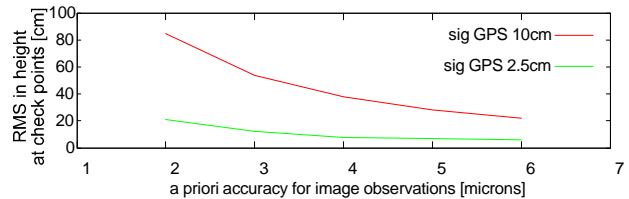


Figure 6. Height accuracy dependency on GPS and image weighting. Block adjustments have been performed without any additional self-calibration parameter set and using AT 4 (see table 2)

Since block adjustment is set up as the described conditions in sub-sections 2.2, 2.3 and 2.4 (GPS weighting, image observations weighting and large number of automatically derived tie points, respectively), presented results should achieve height accuracies comparable to an analogue data, which is not the current case. However, it is possible to overcome with these unexpected large height errors successfully using an appropriate set of additional parameters in the bundle block adjustment.

3.2 Systematic errors in image space

Since the results of section 3.1 suggest that image observations could be influenced by systematic errors, in this sub-section the systematic error in image space is analyzed. By relaxing the *a priori* standard deviations of the image observations these systematic errors, together with effects of other error sources, are projected into image space and can be seen as image residuals in the bundle adjustment. Weighted (inverse of the distance) moving average image residuals in along- and across-track direction are computed from all images of the block, which are visualized in the figure 7. The image residuals have been taken from the AT 4 adjustment (see table 2) using highly weighted GPS observations (2.5 cm, 1- σ) and lowly weighted image observations (6 μm , 1- σ) without self-calibration.

In figure 7 three effects can be observed and can be better understood with figures 8 and 9:

1. A salt-and-pepper pattern that may come from image matching blunders.
2. A low frequency pattern within each image quarter that could be in relation to head calibration issues (fig 8).
3. A high frequency pattern, which could be in relation to manufacturing CCD accuracy issues or other error source (in fig 9 with salt-and-pepper pattern).

The range of the represented residual values is approximately -3 μm to 3 μm in all the four image quarters (in figure 7), which corresponds to a half of the pixel size.

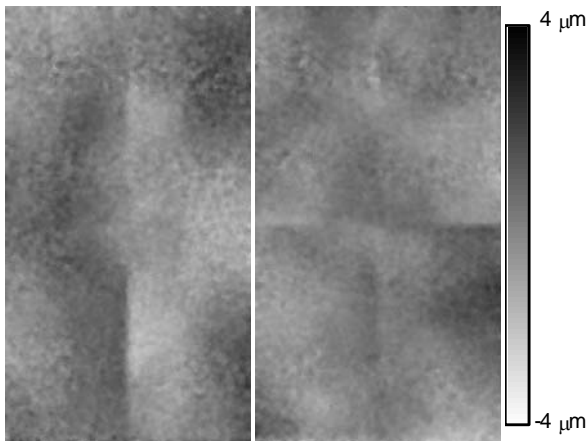


Figure 7. Weighted (inverse of distance) moving average image residuals, left and right images along- and across-track respectively (flight direction rightwards)

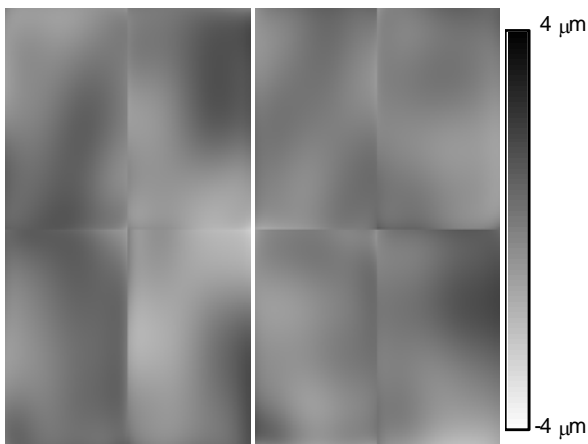


Figure 8. Low frequency systematic error derived from fig. 7, left and right images along- and across-track respectively (flight direction rightwards)

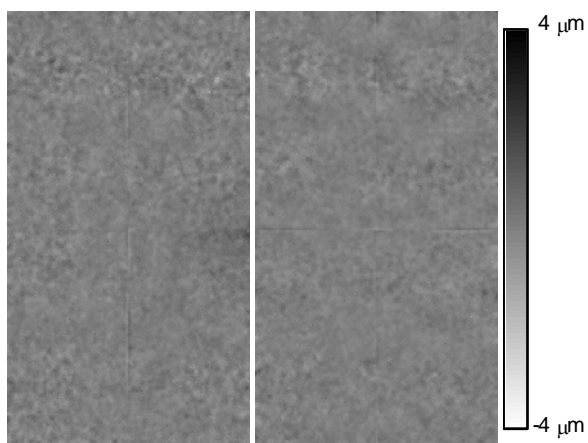


Figure 9. High frequency systematic error derived subtracting fig. 8 from fig. 7, left and right images along- and across-track respectively (flight direction rightwards)

Figure 8 left and right has been derived by minimum least squares approximation using bivariate polynomials of degree 7 per image quarter for the residuals shown in figure 7. This approach has been carried out in order to characterize the low frequency systematic errors and it is not a proposal of additional parameters. Further work should find an adequate

functional model that could better describe this low frequency systematic error.

Figure 9 represents the remaining residuals shown in figure 7 once low frequency systematic errors (figure 8) are subtracted.

3.3 Self-calibration parameters

This sub-section discusses the capability of the 4 sets of 12 self-calibration parameters (Ebner, 1976) to model the low frequency systematic errors in image space.

The weighted mean image residuals in the figure 10 are computed in the same way as those in the figure 7, but here, 4 sets of 12 self-calibration parameters are applied in the bundle adjustment. This approach partly decreases the low frequency systematic error shown in figures 7 and 8 reducing the range of the systematic errors to approximately -1.5 μm to 1.5 μm in each image quarter (see fig. 10). Nevertheless, figure 10 still shows some of the low frequency systematic errors seen in fig. 8 that can not be modelled by a polynomial approach of degree 2 (as the 12 self-calibration parameters). Although the 4 x 12 parameter approach improves significantly the height accuracy (see sub-section 3.1), it is not the most appropriate set of parameters to handle the low frequency systematic errors shown in the figure 8.

Further development should analyze a suitable set of self-calibration parameters that would be able to model the low frequency systematic errors properly.

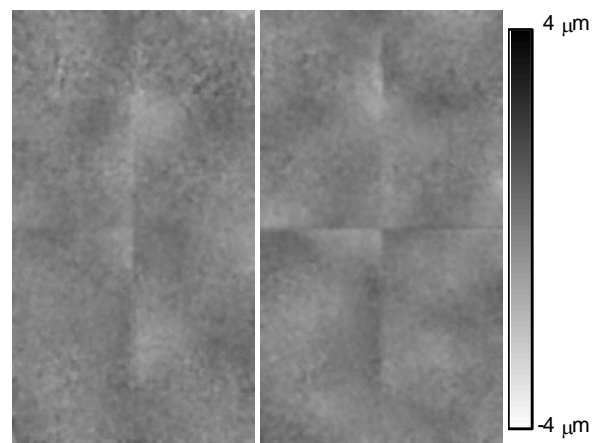


Figure 10. Weighted (inverse of distance) moving average image residuals when 4 sets of 12 self-calibration parameters are used, left and right images along- and across-track respectively (flight direction rightwards)

3.4 Stability of systematic errors in image space

In this sub-section some results on the analysis of low frequency systematic errors in image space are reported computed over 4 data sets (2 of them flown at an altitude of 4 500 m and the other 2 flown at an altitude of 1 000 m approximately). For the complete analysis see (Riesinger, 2007).

In the referenced work it has been evaluated the degree of constancy that mean image residuals have in those 4 data sets. It has been shown that mean image residuals of every block can be reduced up to 60 %, when mean image residuals of all blocks are averaged and subtracted from every block. This

percentage increases up to 80% when the mean image residuals are averaged from the two data sets with similar flying height configuration only. Such results suggest that there is a height dependency on the systematic error in images. Nevertheless, as the low and high altitude flights are taken with a time difference of 3 months it can not be excluded that there is also a time dependent effect.

4. CONCLUSIONS

Theoretical accuracy analysis has proved that the b/h handicap of the DMC is compensated with a higher image pointing accuracy together with accurate GPS observations and a high number of tie point measurements generated by image matching techniques. Theoretically it is possible to achieve comparable height accuracies with the block set ups of analogue cameras.

As in bundle adjustment doubling the accuracy of image pointing does not compensate the reduction by a factor 2 of b/h , a higher accuracy in control and/or GPS data or a high density tie point distribution is required to handle and keep under control the error propagation through the block. Notice that this conclusion is derived only from theory and synthetic data sets. Similar conclusion could be derived for any other camera with a b/h less than 0.6.

For some DMC data sets unexpected large height errors are obtained, especially, if the blocks are highly connected (with a large number of image observations and correspondent object points) and if only poor or even no GPS data observations are available. Nevertheless, self-calibration with 4 independent sets of 12 parameters (one for each image quadrant) in the block adjustment improves significantly the results. This approach is able to model systematic errors well enough to reach the theoretical accuracies and precisions forecasted in published DMC papers.

Two different types of systematic errors in image space are detected: A low frequency systematic errors, that can partially be modelled by the 4 sets of 12 additional parameters and also a high frequency systematic errors. The low frequency could be related to camera head calibration issues, while the high frequency could be related to CCD chip manufacturing precision.

Despite the 4 sets of 12 additional parameters improve significantly the results in block adjustments they are not able to model all the low frequency systematic errors in image space. This requires a higher degree polynomial approach (or a more appropriate functional model) than the second order, which is realized in the 12 parameter model.

The analysis on the stability of the low frequency systematic errors in image space suggests that there could be a height or time dependency. It is critical to prove whether the systematic errors in image space are stable in time and flying height in order to be able to calibrate or characterize systematic errors and also to apply the calibration in the virtual image generation process. If further work will prove non-stability of systematic errors in image space, a suitable and rigorous set of additional parameters has to be derived.

REFERENCES

- Alamús R., et al., 2005. Validation process of the ICC digital Camera. In: *ISPRS Hannover workshop 2005 "High-Resolution Earth Imaging for Geospatial Information"*, 17-20th May 2005, Hannover (Germany).
- Alamús R., Kornus W., Talaya J., 2006. Studies on DMC geometry. In: *ISPRS Journal of Photogrammetry & Remote Sensing*, V 60, issue 6, pp 375-386. Elsevier B.V..
- Cramer M., 2007. Presentation of DMC related test results at Intergraph ZI European DMC User Meeting, Gävle, Sweden, January 30-31, 2007. <http://www.ifp.uni-stuttgart.de/euroedr/Gaevle07-EuroSDR-DMC.pdf>
- Dörstel, C., 2003. DMC- Practical Experiences and Photogrammetric System Performance. In: *Photogrammetric Week 2003* Fritsch D. (Ed.), September 2003 Stuttgart (Germany), pp. 59-65.
- Ebner, H., 1976. Self-calibrating block adjustment. In: *Congress of the International Society for Photogrammetry*. Invited paper of Commission III, 1976, Helsinki (Finland).
- Hefele J., Dörstel C., 2007. Mid Exposure Pulse versus Start Exposure Pulse. Report distributed to the DMC User Network.
- Hinz A., 1999. The Z/I Digital Aerial Camera System. In: *Proceedings of the 47th Photogrammetric Week*. 1999, Stuttgart (Germany), pp. 109-115.
- Honkavaara E., et al. 2006a. Geometric test field calibration of digital photogrammetric sensors. In: *ISPRS Journal of Photogrammetry & Remote Sensing*, V 60, issue 6, pp 387-399. Elsevier B.V..
- Honkavaara E., et al. 2006b. Theoretical and empirical evaluation of geometric performance of multi-head large format photogrammetric sensors. In: ISPRS Commission I Symposium – Paris 2006 "From sensors to imagery", on CD-Rom.
- Riesinger I., 2007. Investigations on DMC (Digital Metric Camera) Auto-Calibration. Diploma thesis at Technical University Munich (TUM). Not published.
- Schroth R.W., 2007. Large format digital cameras for aerial survey of geospatial information. In: *FIG Working Week 2007*. Hong Kong SAR, China 13-17 May 2007.
- Zeitler, W., Dörstel, C., Jacobsen, K., 2002. Geometric Calibration of the DMC: Method and Results. In: *IntArchPhRs*, Com. I, Denver (USA), Vol XXXIV Part 3b, pp 324-333.